Dose-Response:
An International Journal
April-June 2021:1-6

DOI: 10.1177/15593258211011359
journals.sagepub.com/home/dos
SAGE

Investigating Dual-Energy CT Post-Contrast Phases for Liver Iron Quantification: A Preliminary Study

Luca Basso[1], Dario Baldi[1], Lorenzo Mannelli[1], Carlo Cavaliere[1], Marco Salvatore[1], and Valentina Brancato[1]

Abstract

Background and Purpose: Quantification of hepatic virtual iron content (VIC) by using Multidetector Dual Energy Computed Tomography (DECT) has been recently investigated since this technique could offer a good compromise between accuracy and non-invasiveness for liver iron content quantification. The aim of our study is to investigate differences in VIC at different DECT time points (namely baseline and arterial, venous and tardive phases), identifying the most reliable and also exploring the underlying temporal trend of these values.

Materials and Methods: Eleven patients who underwent DECT examination and were characterized by low liver fat content were included in this retrospective study. By using the Syngo.via Frontier–DE IronVNC tool, regions of interest (ROI) were placed on the VIC images at 3 hepatic levels, both in left and right liver lobes, at each DECT time point. Friedman's test followed by Bonferroni-adjusted Wilcoxon signed-rank test for post-hoc analysis was performed to assess differences between DECT timepoints. Page's L test was performed to test the temporal trend of VIC across the 4 examined timepoints.

Results: For both liver lobes, Friedman's test followed by Bonferroni-adjusted Wilcoxon signed-rank test revealed that VIC values differed significantly when extracted from ROIs placed at the 4 different timepoints. The Page's L test for multiple comparison revealed a significant growing trend for VIC, from baseline acquisition to the fourth and last time point post-contrast agent injection.

Conclusions: The extraction of hepatic VIC in healthy subjects was found to be significantly influenced by the DECT time point chosen for the extrapolation of the VIC values.

Keywords
DECT, liver iron load, VIC, triphasic

Introduction

Iron is a biologically essential element of the oxygen carriers and other enzymes that are involved in the oxidation or reduction of biological substrates. The liver is a major site of iron storage and is highly vulnerable to injury from iron overload.[1] In the healthy liver, iron is present at a concentration lower than 20 μmol/g of dry weight. However, the increase of liver iron content (LIC) can occur in a variety of conditions, including the presence of hepatic diseases such as early genetic hemochromatosis, non-transfused dysmyelopoiesis, hereditary aceruloplasminemia, iron overload secondary to cirrhosis, mixed iron overload, insulin resistance syndrome, ferroportin disease, hepatitis C or B, porphyria cutanea tarda, late genetic hemochromatosis, and inflammatory syndrome.[2-4]

The assessment of LIC is still associated with histochemical or biochemical evaluation using liver biopsy, which is

[1] IRCCS SDN, Naples, Italy

Received 13 January 2021; received revised 17 March 2021; accepted 29 March 2021

Corresponding Author:
Dario Baldi, IRCCS SDN, via E. Gianturco 113, 80143 Naples, Italy.
Email: dario.baldi@synlab.it

considered the most reliable method to calculate iron amount within organs. However, the high invasiveness, together with the need for patient hospitalization and the high cost for the patient, are the main drawbacks of this method. Therefore, in recent years, there has been increasing interest in investigating non-invasive techniques substituting liver biopsy and capable of providing an accurate LIC assessment. Several Magnetic Resonance Imaging (MRI)-based techniques have proven to be useful for this purpose.[5] However, in the last decade, with the advent of the Multidetector Dual Energy Computed Tomography (DECT) technique and the related DE-based material decomposition, Computed Tomography (CT) has evolved into an alternative to MRI for quantifying LIC, with the benefit of being more easily accessible and requiring shorter examination times.[3,6-9]

DECT is one of the latest innovations in the field of liver CT imaging. Based on the acquisition of 2 simultaneous X-ray beams with different energy levels, DECT enables the characterization of the scanned tissues by using imaging-based algorithms able to discriminate materials on the basis of their interactions with photons.[10-13] Since the absorption coefficients of different materials have a different dependence on energy, it is possible to obtain images in which a specific material appears completely transparent to X radiation and generate virtual non-contrast (VNC) images in acquisition obtained post intravenous contrast.[14] Material-specific images may be used to determine the presence and quantity of materials with unique absorption characteristics, including iron. By using an iron-specific 3-material decomposition algorithm, Virtual Iron Content (VIC) imaging at dual-energy CT could enable an accurate quantification of LIC, offering the best compromise between accuracy and non-invasiveness.[15,16]

Previous studies aimed at quantifying LIC stratification using virtual iron concentration (VIC) imaging on DECT in patient populations with different liver pathologies, finding promising results either in an in-vivo or an ex-vivo setting.[3,17,18]

Specifically, an ex-vivo phantom study by Fischer et al indicated that hepatic VIC imaging on DECT could allow for an accurate quantification of LIC.[17] Moreover, Werner et al found that hepatic VIC was useful for quantification of LIC in patients with hematological disorders, suggesting its use in the clinical routine for evaluation of transfusional hemosiderosis.[3] Also, Luo et al found that hepatic VIC was a potential tool for accurately assessing and grading clinically relevant liver iron accumulation.[18]

As reported in the same study, iron enhancement is similar to iodine enhancement at contrast material–enhanced CT. Thus, hepatic VICs could reflect changes in liver iron concentration. It remains to be studied if variations in hepatic VIC may occur when considering post-contrast scans, as well as if these values may be associated with the delay between post-contrast and baseline scans, which, to date, is the most commonly used sequence for LIC evaluation using VIC images.[18-20]

Therefore, the aim of this study is to investigate differences in VIC values at different DECT time points (namely baseline, arterial, venous and tardive).

Materials and Methods

Patient Population

This retrospective study was approved by the institutional review board, with waiver of informed consent.

A total of 15 healthy adult patients who underwent contrast-enhanced abdominal DECT, examined at IRCCS SDN, Naples (IT), from January 1, 2020 to February 29, 2020, were included. The selected patients did not show any liver disease or any pathologies that could have repercussions on the liver state of health. Inclusion criteria were the following: patient's age >18 years, liver fat content <5%. Since 5% is considered the fat fraction threshold above which the hepatic steatosis is considered not negligible, 4 patients with fat levels above 5% were excluded.[21,22]

DECT Data Acquisition

All patients underwent DECT with a third-generation dual source multidetector CT scanner (Somatom Force, Siemens Healthineers, Germany). To perform the exam, all patients observed a fasting period of at least 8 hours and showed a correct value of renal filtration. The protocol included an unenhanced spiral CT of the liver, performed before contrast injection. For the triphasic spiral CT scans, the liver was scanned in the arterial (25 sec delay), portal-venous (70 sec delay) and tardive phase (180 sec delay) of liver perfusion, and each of the scans was acquired in dual energy mode. By using an automatic injector, 100 mL of Iopamiro (370 mg/mL, Iopamidol, Bracco, Italy) followed by 30 mL of saline flush was injected into an ante-cubital vein at a flow rate of 4.0 mL/s. Scan parameters were the following: collimation $2 \times 192 \times 0.625$ mm; large FOV; pitch 0.6; 150/100 kVp. The virtual 120 kVp images were generated by linearly blending data from both detectors. In particular, 60% of information from the scan was obtained using 100 kVp and 40% using Sn 150 kVp with a 0.6 weighting factor, in accordance with manufacturer-recommended standard settings. These blended images resemble the image quality of a conventional single-energy CT acquisition at 120 kVp.[23,24]

Automated attenuation-based anatomical tube current (mAs) modulation CARE Dose4D (Siemens Healthineers) and automated attenuation-based tube voltage (kV) selection functionality CARE kV (Siemens Healthineers) were used for dose reduction and optimization.[25] Data were reconstructed with a third-generation Advanced Modeled Iterative REconstruction (ADMIRE, Siemens Healthineers) and a dedicated IBHC algorithm for the correction of the beam hardening that improved image quality using 3D forward projection and exploits an additional 2-compartment iodine/water model. ADMIRE was

set at a strength level of 3 (range 1-5) with medium smooth reconstruction convolution kernel (Bv40).

DECT Image Reconstruction

All images were reconstructed by 2 radiologists who were not involved in the CT data analysis.

For each patient, the following 5 sets of images were reconstructed: 100 kV images acquired during DECT; 150 kVp images acquired during DECT; Linearly blended images using a 50%:50% weighted ratio of the 100 kVp and 150 kVp dual-energy data; VIC images derived from dual-energy 3-material decomposition, using DECT data acquired at 100 kVp and 150 kVp; FATMAP–Virtual non-contrast (VNC) images derived from dual-energy 3-material decomposition, using DECT data acquired at 100 kVp and 150 kVp.

Dual-energy 3-material decomposition was performed to separate fat, liver tissue, and iron by using commercially available post-processing software (Liver virtual non-contrast (VNC), syngo Dual Energy, Siemens AG, Forchheim, Germany). The liver VNC application enables the visualization of iodine contrast agent concentration in the liver without a supplementary non-contrast scan, even in the presence of irregular fatty infiltration of the liver or necrotic areas. Briefly, the sum of masses of the 3 constituent materials is equivalent to the mass of the mixture. With this assumption, it is possible to solve an equation for 3 unknown variables with only 2 spectral measurements, using a mass-conservation based 3-material decomposition DECT algorithm.[16]

Data Analysis

In order to select patient with liver fat content <5%, the hepatic fat fraction (%) was evaluated on a dedicated workstation (CT Dual Energy–Syngo.via, VB30A_HF06, Siemens Healthineers) by using the fat map obtained from the Virtual Non-Contrast image by linear rescaling and applying a weak noise reduction filter. The base material soft tissue corresponds to 0% fat, while the base material fat to 100% fat. Hepatic fat fraction was measured on the non-enhanced scan by a radiologist with 8 years of experience in abdomen CT imaging. A free hand region-of-interest (ROI) segmentation approach was used. Specifically, the right and left hepatic lobes were segmented using the hepatic hilum as first reference point and being careful to exclude the large vessels and keeping a distance of 1 cm from the outer margin of the liver. Subsequently, this operation was repeated by moving first 4 cm cranially from the reference point, and then again 4 cm caudally, obtaining 3 ROIs for each hepatic lobe.

After this step, DECT images of included patients were transferred for post-processing to a vendor-provided workstation and by using the research tool by Syngo.via Frontier–DE IronVNC (Siemens Healthineers, version n. 1.1.0) for the automatic quantification of VIC (mg/mL). A base material map of hepatic iron, water and air was generated for extraction of VIC values. The same segmentation approach was used. VIC values were extracted from scans acquired pre- and post-injection of the contrast agent, keeping ROI size, shape, and position constant among the 4 DECT phases and visually colocalizing ROIs in each contrast phase at the workstation.

Statistical Analysis

A mean-based approach was used to perform VIC analysis. Specifically, for each patient, the mean value of VIC across the 3 ROIs was computed. This was performed for both left and right liver lobes, separately.

The comparison among the mean values of VIC extracted from ROIs on the non-enhanced scan and on the 3 different post-contrast scans was performed using the Friedman's test followed by Bonferroni-adjusted Wilcoxon signed-rank test for post-hoc analysis, carrying out a separate analysis of the values obtained in the left and right lobes. Furthermore, Page's L test[20] was performed to test the temporal trend of VIC across the 4 examined timepoints. A probability value of $P < 0.05$ was considered significant in all analyses. Statistical analysis was performed using Matlab R2020a (The MathWorks Inc., Natick, MA, USA).

Results

Figure 1 shows how the ROIs have been positioned for the extraction of VIC values. Due to the physiological conformation of the liver in 9 of the 11 patients studied it was not possible to assess in the left lobe the level of iron at the most caudal slice. Conversely, in 2 of the 11 patients considered, the liver volume was higher and this allowed the extraction of VIC values. Mean values of VIC ($\pm$standard deviation) at each different time point and for each liver lobe, as well as results of multiple comparisons, are reported in Table 1.

For both liver lobes, Friedman's test revealed that significant differences existed between VIC values associated with the 4 DECT timepoints. Post hoc Bonferroni-adjusted Wilcoxon signed-rank test revealed significant differences in VIC values among each pair of timepoints. In particular, in both liver lobes, VIC values at baseline were significantly lower than VIC values at all post-contrast phases. VIC values at arterial phase were significantly higher than those at baseline, and significantly lower than those found at the venous and tardive phase. VIC values at the venous phase were significantly higher than those at the other 3 time points, while VIC values at the tardive phase were significantly higher than those at baseline and the arterial phase, but lower than the venous phase. The Page's L test for multiple comparisons revealed a significant growing trend for VIC, from baseline acquisition to the fourth and last time point post-contrast agent injection ($P < 0.001$).

Discussion

In this study, we investigated differences in hepatic VIC values obtained at baseline and the subsequent 3 post-contrast phases

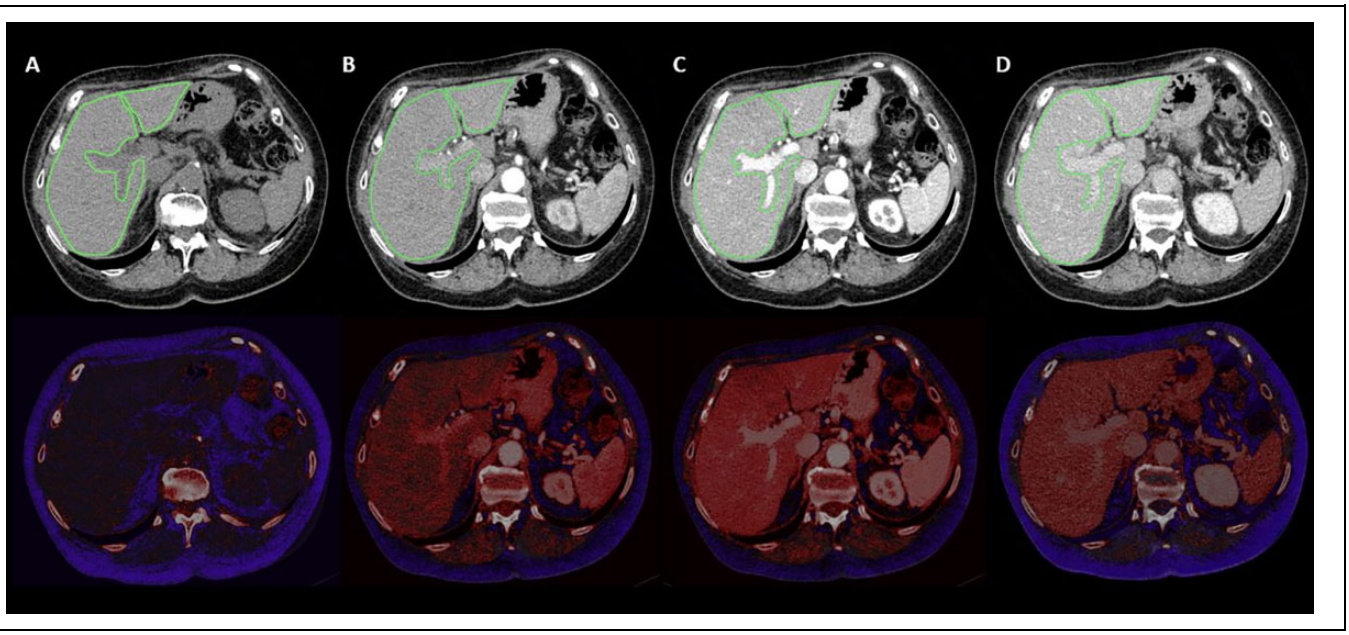

Figure 1. On the first row, example of region of interest (ROIs) placement for right and left liver lobes on baseline (A), arterial (B), portal (C) and tardive (D) DECT phase. On the second row, the corresponding iron map generated with the DE IronVNC software. The measured values of hepatic iron are [mg/mL]: baseline 1.36 (R)-0.85 (L); arterial 3.57 (R)-4.26 (L); portal 14.1 (R)-13.54 (L); tardive 14.08 (R)-13.48 (L). DECT, dual energy computed tomography; VIC, virtual iron content; R, right lobe; L, left lobe.

Table 1. Mean Values ± Standard Deviation of Virtual Iron Content (VIC) [mg/mL] at Basal and Post-Contrast Injection Timepoints, Both in Right and Left Lobes.

Liver lobe	Basal (tp1)	Arterial (tp2)	Venous (tp3)	Tardive (tp4)
Right	1.51 ± 0.35*°§	5.41 ± 1.38^°§	12.02 ± 3.19^*§	8.48 ± 2.71^*°
Left	1.45 ± 0.52*°§	5.58 ± 1.28^°§	12.5 ± 2.42^*§	9.08 ± 2.42^*°

Abbreviations: tp1, time point 1; tp2, time point 2; tp3, time point 3; tp4, time point 4.
Notes: ^Significantly different from tp1; *significantly different from tp2; °significantly different from tp3; §significantly different from tp4. Significant *P*-values were $P < 0.005$ according to Bonferroni correction.

(namely arterial, venous and tardive) on DECT images and explored the temporal trend of VIC across the 4 examined timepoints. The analysis was performed in both liver lobes. According to our results, the extraction of the hepatic VIC in healthy subjects was found to be significantly influenced by the phase chosen for the extrapolation of the VIC values. It could be inferred from the considerably different VIC values associated with each DECT phase. The same behavior could be observed in both liver lobes. Our results revealed that VIC values differed significantly when extracted from ROIs placed at baseline and the subsequent 3 post-contrast phases. In particular, the non-enhanced scan was associated with the lowest VIC values, while in the portal-venous scan was associated with the highest VIC values. Interestingly, although hepatic VIC values at the tardive phase were significantly higher than those at baseline and the arterial phase, but lower than the portal phase, a significant growing trend for hepatic iron values, from baseline acquisition to the fourth and last time point post-contrast agent injection was found.

The selection of healthy subjects with lower liver fat percentage, together with their observation of a fasting period of at least 8 hours, has allowed us to obtain data that is as faithful to reality as possible, thereby overcoming the intersubjective variability in the inherent liver attenuation, that turns out to be the main limitation and the dominant source of uncertainty of measurement of hepatic iron.[3,26]

Moreover, we used the same iron-specific algorithm used by Fischer et al in a phantom study on iron-specific algorithm-based VIC images obtained with dual-energy analysis by using mixed veal liver with iron at titrated iron concentrations.[8]

It should be noted that fat could be a confounding factor in the estimation of hepatic iron. However, as shown in an ex-vivo phantom study, iron-specific algorithm-based VIC imaging could eliminate the fat confounding effect.[17] Moreover, a recent animal study showed that coexisting hepatic iron and fat could be separated with dual-energy CT using the iron-specific 3-material decomposition algorithm.[19] Despite these early results, fat confounding effect should be further studied

in patients with iron overload. Since we did not examine patients with coexisting iron and fat, we could not assess iron estimation in the presence of fat. However, it could be interesting to quantify the percentage of liver fat, since the ability of DECT to quantify fat within the abdomen is also of great interest.[27,28]

To our knowledge, this is the first study on DECT aiming at evaluating hepatic VIC at post-contrast agent injection and comparing these values with hepatic VIC values at baseline.

Although the novelty of the used approach, this study suffers from some limitations. First, the patient population was very small. However, this study must be considered as a preliminary study aiming to offer a new possibility of getting valuable information on hepatic iron content. Second, since iron enhancement is similar to iodine enhancement at contrast material–enhanced CT,[8,18] it is true to say that hepatic VICs could reflect changes in liver iron concentration. However, it should be considered that our measurements could be affected by the influence of iodine enhancement. Therefore, future studies investigating the possibility to extract hepatic iron without iodine influence are required. It could be also interesting to investigate the possibility to extract VIC from VNC reconstruction. It could have a significant impact on clinical practice mainly due to the lower radiation dose characterizing VNC by obviating need for true non contrast images.[29] Then, iron quantification was not performed in the whole liver, but at 3 levels, assuming the hepatic hilum as initial reference, and then moving 4 cm cranially and 4 cm caudally. Although a complete volumetric coverage of the liver would provide a global assessment of VIC values, our segmentation approach was considered to be appropriate since it involves the ROI placement on nonconsecutive slice locations, the exclusion of blood vessels and the coverage of both right and left lobe considering the largest possible freehand ROIs.[3,18,30,31] Finally, we did not have a histologic reference for our data, and this did not allow us to perform a correlation analysis between VIC and LIC, as done by Luo et al and Xie et al.[32,33]

In conclusion, our preliminary study showed that the extraction of the VIC in healthy subjects was significantly influenced by the DECT time point chosen for the extrapolation of the VIC values. Although further studies are required to confirm our preliminary findings, our study provides new insights concerning the role of DECT technique and its utility for hepatic iron quantification.

Authors' Note

The opinions expressed in the presented article are our own and not an official position of the institution or funder.

Declaration of Conflicting Interests

The author(s) declared no potential conflicts of interest with respect to the research, authorship, and/or publication of this article.

Funding

The author(s) received no financial support for the research, authorship, and/or publication of this article.

ORCID iD

Dario Baldi https://orcid.org/0000-0001-7464-4499
Lorenzo Mannelli https://orcid.org/0000-0002-9102-4176

References

1. Ganz T. Molecular control of iron transport. *JASN*. 2007;18(2):394-400. doi:10.1681/ASN.2006070802
2. Batts KP. Iron overload syndromes and the liver. *Mod Pathol*. 2007;20(S1):S31-S39. doi:10.1038/modpathol.3800715
3. Werner S, Krauss B, Haberland U, et al. Dual-energy CT for liver iron quantification in patients with haematological disorders. *Eur Radiol*. 2019;29(6):2868-2877. doi:10.1007/s00330-018-5785-4
4. Labranche R, Gilbert G, Cerny M, et al. Liver iron quantification with MR imaging: a primer for radiologists. *RadioGraphics*. 2018;38(2):392-412. doi:10.1148/rg.2018170079
5. Hernando D, Levin YS, Sirlin CB, Reeder SB. Quantification of liver iron with MRI: state of the art and remaining challenges. *J Magn Reson Imaging*. 2014;40(5):1003-1021. doi:10.1002/jmri.24584
6. Tsai Y-S, Chen J-S, Wang C-K, et al. Quantitative assessment of iron in heart and liver phantoms using dual-energy computed tomography. *Exp Ther Med*. 2014;8(3):907-912. doi:10.3892/etm.2014.1813
7. Schena E, Liguori C, Frauenfelder G, et al. Emerging clinical applications of computed tomography. *MDER*. Published online June 2015:265. doi:10.2147/MDER.S70630
8. Fischer MA, Reiner CS, Raptis D, et al. Quantification of liver iron content with CT—added value of dual-energy. *Eur Radiol*. 2011;21(8):1727-1732. doi:10.1007/s00330-011-2119-1
9. Ma Q, Hu J, Yang W, Hou Y. Dual-layer detector spectral CT versus magnetic resonance imaging for the assessment of iron overload in myelodysplastic syndromes and aplastic anemia. *Jpn J Radiol*. 2020;38(4):374-381. doi:10.1007/s11604-020-00921-9
10. Coursey CA, Nelson RC, Boll DT, et al. Dual-energy multidetector CT: how does it work, what can it tell us, and when can we use it in abdominopelvic imaging? *Radiographics*. 2010;30(4):1037-1055. doi:10.1148/rg.304095175
11. Agrawal MD, Pinho DF, Kulkarni NM, Hahn PF, Guimaraes AR, Sahani DV. Oncologic applications of dual-energy CT in the abdomen. *Radiographics*. 2014;34(3):589-612. doi:10.1148/rg.343135041
12. Johnson TRC. Dual-energy CT: general principles. *Am J Roentgenol*. 2012;199(5_supplement):S3-S8. doi:10.2214/AJR.12.9116
13. De Cecco CN, Darnell A, Rengo M, et al. Dual-energy CT: oncologic applications. *Am J Roentgenol*. 2012;199(5_supplement):S98-S105. doi:10.2214/AJR.12.9207
14. Marin D, Boll DT, Mileto A, Nelson RC. State of the art: dual-energy CT of the abdomen. *Radiology*. 2014;271(2):327-342. doi:10.1148/radiol.14131480
15. Laukamp KR, Ho V, Obmann VC, et al. Virtual non-contrast for evaluation of liver parenchyma and vessels: results from 25 patients using multi-phase spectral-detector CT. *Acta Radiol*. 2020;61(8):1143-1152. doi:10.1177/0284185119893094

16. Liu X, Yu L, Primak AN, McCollough CH. Quantitative imaging of element composition and mass fraction using dual-energy CT: three-material decomposition. *Med Phys*. 2009;36(5):1602-1609. doi:10.1118/1.3097632
17. Fischer MA, Gnannt R, Raptis D, et al. Quantification of liver fat in the presence of iron and iodine: an ex-vivo dual-energy CT study. *Invest Radiol*. 2011;46(6):351-358. doi:10.1097/RLI.0b013e31820e1486
18. Luo XF, Xie XQ, Cheng S, et al. Dual-energy CT for patients suspected of having liver iron overload: can virtual iron content imaging accurately quantify liver iron content? *Radiology*. 2015;277(1):95-103. doi:10.1148/radiol.2015141856
19. Ma J, Song Z-Q, Yan F-H. Separation of hepatic iron and fat by dual-source dual-energy computed tomography based on material decomposition: an animal study. *PLoS ONE*. 2014;9(10):e110964. doi:10.1371/journal.pone.0110964
20. Page EB. Ordered hypotheses for multiple treatments: a significance test for linear ranks. *J Am Stat Assoc*. 1963;58(301):216-230. doi:10.1080/01621459.1963.10500843
21. Graffy PM, Sandfort V, Summers RM, Pickhardt PJ. Automated liver fat quantification at nonenhanced abdominal CT for population-based steatosis assessment. *Radiology*. 2019;293(2):334-342. doi:10.1148/radiol.2019190512
22. Pickhardt PJ, Graffy PM, Reeder SB, Hernando D, Li K. Quantification of liver fat content with unenhanced MDCT: phantom and clinical correlation with MRI proton density fat fraction. *Am J Roentgenol*. 2018;211(3):W151-W157. doi:10.2214/AJR.17.19391
23. Durieux P, Gevenois PA, Muylem AV, Howarth N, Keyzer C. Abdominal attenuation values on virtual and true unenhanced images obtained with third-generation dual-source dual-energy CT. *Am J Roentgenol*. 2018;210(5):1042-1058. doi:10.2214/AJR.17.18248
24. Yeh BM, Shepherd JA, Wang ZJ, Seong Teh H, Hartman RP, Prevrhal S. Dual-energy and low-kVp CT in the abdomen. *Am J Roentgenol*. 2009;193(1):47-54. doi:10.2214/AJR.09.2592
25. Baldi D, Tramontano L, Alfano V, Punzo B, Cavaliere C, Salvatore M. Whole body low dose computed tomography using third-generation dual-source multidetector with spectral shaping: protocol optimization and literature review. *Dose-Response*. 2020;18(4):155932582097313. doi:10.1177/1559325820973131
26. Wood JC, Mo A, Gera A, Koh M, Coates T, Gilsanz V. Quantitative computed tomography assessment of transfusional iron overload. *Br J Haematol*. 2011;153(6):780-785. doi:10.1111/j.1365-2141.2011.08590.x
27. Artz NS, Hines CDG, Brunner ST, et al. Quantification of hepatic steatosis with dual-energy computed tomography: comparison with tissue reference standards and quantitative magnetic resonance imaging in the ob/ob mouse. *Invest Radiol*. 2012;47(10):603-610. doi:10.1097/RLI.0b013e318261fad0
28. Martin SS, Weidinger S, Czwikla R, et al. Iodine and fat quantification for differentiation of adrenal gland adenomas from metastases using third-generation dual-source dual-energy computed tomography. *Invest Radiol*. 2018;53(3):173-178. doi:10.1097/RLI.0000000000000425
29. Si-Mohamed S, Dupuis N, Tatard-Leitman V, et al. Virtual versus true non-contrast dual-energy CT imaging for the diagnosis of aortic intramural hematoma. *Eur Radiol*. 2019;29(12):6762-6771. doi:10.1007/s00330-019-06322-5
30. Abadia AF, Grant KL, Carey KE, Bolch WE, Morin RL. Spatial distribution of iron within the normal human liver using dual-source dual-energy CT imaging. *Invest Radiol*. 2017;52(11):693-700. doi:10.1097/RLI.0000000000000393
31. Joe E, Kim SH, Lee KB, et al. Feasibility and accuracy of dual-source dual-energy CT for noninvasive determination of hepatic iron accumulation. *Radiology*. 2012;262(1):126-135. doi:10.1148/radiol.11110060
32. Luo XF, Yang Y, Yan J, et al. Virtual iron concentration imaging based on dual-energy CT for noninvasive quantification and grading of liver iron content: an iron overload rabbit model study. *Eur Radiol*. 2015;25(9):2657-2664. doi:10.1007/s00330-015-3693-4
33. Xie T, Li Y, He G, Zhang Z, Shi Q, Cheng G. The influence of liver fat deposition on the quantification of the liver-iron fraction using fast-kilovolt-peak switching dual-energy CT imaging and material decomposition technique: an in vitro experimental study. *Quant Imaging Med Surg*. 2019;9(4):654-661. doi:10.21037/qims.2019.04.06